УДК 577.181.5

SOME SIGNAL EFFECTS IN HUMAN ERYTHROCYTES ON SPECIFIC BINDING OF FREE DOXORUBICIN AND DOXORUBICIN CONJUGATES WITH MAGNETITE NANOPARTICLES

O. M. MYKHAYLYK[1], A. V. KOTSURUBA[2], N. O. DUDCHENKO[1], G. TÖROK[3]

[1]Інститут прикладних проблем фізики і біофізики НАН України, Київ;
[2]Інститут біохімії ім. О. В. Палладіна НАН України, Київ;
[3]Інститут фізики твердого тіла і оптики, Будапешт, Угорщина;
e-mail:diu@cyfra.net, olga.mykhaylik@gmx.net

В роботі досліджено зв'язування іммобілізованого на поверхні нанодисперсного магнетиту (М) доксорубіцину (ДОКС) з інтактними еритроцитами людини в конкуренції з вільним ДОКС для кон'югатів (ДОКС-М) із концентрацією іммобілізованого ДОКС у діапазоні 0,16–25,1 мг/г носія. Виявлено наявність двох місць специфічного зв'язування ДОКС на плазматичній мембрані еритроцитів. Зміни у впорядкованості наночасточок ДОКС-М-кон'югату, які виявлено методом малокутового розсіювання нейтронів також свідчать про специфічне зв'язування ДОКС-М на поверхні еритроцитів. Вільний ДОКС і ДОКС-М модулюють аналогічні сигнальні ефекти, що виявляється у стимуляції продукції NO та cGMP і, навпаки, у пригніченні продукції cAMP. Дослідження кислотного гемолізу "окислених" еритроцитів показало істотну стабілізацію їхньої мембрани під час зв'язування як вільного ДОКС, так і його магнітних кон'югатів.

К л ю ч о в і с л о в а: доксорубіцин (адріаміцин), кон'югат, еритроцити людини, плазматична мембрана, сигнальна трансдукція, малокутове розсіювання нейтронів, оксид азоту, циклічні пуринові нуклеотиди, кислотний гемоліз.

Doxorubicin (DOX), whose principle target was previously thought to be DNA, has been shown to exert its cytotoxic action solely by cell surface interaction since extracellular drug was required to initiate the cytotoxic reactions [1 , 2]. These findings initiated researches with DOX conjugates to find more efficient drug forms and to reduce the toxicity of free DOX. Nowadays, the increasing evidence firmly suggests that the underlying mechanism for anthracycline cytotoxicity is the induction of apoptosis through intracellular-mediated signaling pathways [3 , 4]. It has also been shown that adriamycin inhibits growth-related NADH oxidase of the plasma membrane of cancer cells associated with apoptosis [5]. Nevertheless, the events in DOX-induced apoptosis are poorly understood and determining the mechanisms of DOX membrane effects remains a challenge.

The purpose of this work was to investigate the binding of DOX, immobilized on a magnetic nanomaterial, to intact human erythrocytes, and to test the effects of this conjugate on signal transduction in human erythrocytes using quantitative determination of the intracellular cAMP and cGMP pools and the stable nitric oxide metabolite – NO_2^-. Human erythrocytes were chosen as a model cell system due to the known interactions of DOX with blood components. These interactions determine, to a great extent, DOX pharmacokinetics [6]. The DOX-erythrocytes binding mechanisms include the imbedding of DOX into the lipid matrix, the insertion of DOX into the erythrocytes stroma using the "flip-flop" mechanism [7], or, depending on the level of cholesterol in the membrane, using a specific transporter [8].

Materials and Methods

All chemicals were purchased from «Sigma-Aldrich», Germany. Nanodispersed magnetite was modified by oligomerization of γ-aminopropyltriethoxysilane and activated with 1,6-diisocyanatohexane as described in [9], followed by chemisorption of hydroxyethylstarch from aqueous solution and repeated activation with 1,6-diisocyanatohexane. The mean diameter of the particle core was 24 ± 19 nm according to electron microscopy data (Fig. 1) and the average nanocrystal size was 30 nm, as calculated from the broadening of the main magnetite peak in the X-ray diffraction pattern.

To synthesize a set of doxorubicin magnetic conjugates (DOX-M), DOX was chemisorbed on the surface of the activated nanocarrier from aqueous solution, pH 6.0, followed by chemisorption of O-(2-aminoethyl)polyethylene glycol 3000 (APEG) from 2.5% water solution. The activated carrier with chemisorbed APEG was used as a reference sample. The concentration values of immobilized DOX in

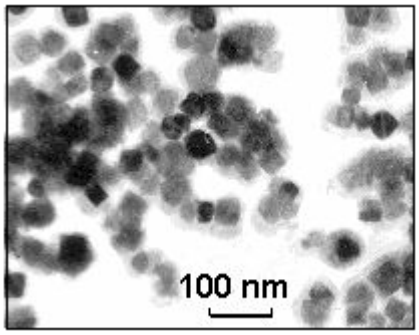

Fig. 1. Electron micrograph of the DOX-M conjugate sample.

DOX-M conjugates were estimated from the decrease in optical density of the contact solutions at $\lambda = 486$ nm, $\varepsilon = 7500$ $M^{-1} \cdot cm^{-1}$ and found to be 0.16; 0.4; 1.2; 6.1 and 25.1 mg DOX/g activated carrier, respectively. The cytotoxicity of conjugated DOX in vitro against A2780 human ovarian carcinoma and KB human epidermoid oral cavity cancer cell lines was close to that of the free DOX. For example, for the conjugate with 6.1 mg immobilized DOX/g carrier, IC_{50} is equal to 2.3 ± 0.2 and $6.9 \pm \pm 0.2$ ng of immobilized DOX/ml compared to $3.4 \pm \pm 0.2$ and 6.4 ± 0.4 ng of free DOX/ml, against A2780 and KB cancer cell lines, respectively.

Packed erythrocytes from three different donors were washed twice with physiological saline using a commonly accepted method based on differential centrifugation. To study DOX-M conjugate binding, washed erythrocytes ($5 \cdot 10^7$ cells/ml of incubation medium) were pre-incubated for 30 min and aliquots of the DOX solutions in physiologic saline were added to achieve final DOX concentrations in the range of 10^{-12}—10^{-5} M. This erythrocyte solution was incubated at 37 °C with gentle agitation for 15 min. Thereafter, 0.1 ml portions of the DOX-M suspensions were added to the mixture, resulting in a ratio *conjugate particles : erythrocyte* of $4 \cdot 10^3$. Samples were incubated for 15 min at 37 °C with gentle agitation followed by magnetic separation of the DOX-M conjugate-labeled cells using a permanent magnet. We measured the optical density of the supernatant at 532 nm (D_{532}) to determine concentration of erythrocytes remaining in suspension. The percentage of cells binding magnetic carrier particles was defined by the decrease in cell concentration in the supernatant, after magnetically separating cells, as: $(1 - D_{532}/D_{532}{}^0)$,%). Each concentration point represents the mean of nine measurements (three independent measurements for erythrocytes from three different donors).

DOX-M nanoparticles ordering in the erythrocytes suspension was investigated by small angle neutron scattering (SANS), which was performed on frozen erythrocyte suspensions at −10 °C using a "Yellow Submarine" spectrometer at the Budapest Neutron Center ($\lambda = 0.408$ and 0.816 nm). A linear chain model was used to fit the data. DOX-M conjugate samples with 6.1 mg immobilized DOX/g carrier were measured. A DOX-M suspension in physiological saline was added to the wasched erythrocyte suspension (hematocryte index = 0.4) at 37 °C, at a final concentration $3.2 \cdot 10^3$ conjugate particles per cell and frozen immediately (sample *a*), after a 10 min incubation (sample *b*), or after a 30 min incubation (sample *c*). Another erythrocyte sample was preincubated for 10 min in the presence of 0.2 μM free DOX to saturate binding sites, then the DOX-M suspension was introduced as above, and frozen after a 30 min incubation (sample *d*).

To test the effects of the preparations on signal transduction by human erythrocytes, a suspension of $5 \cdot 10^7$ cells per ml was quickly mixed with aliquot of free or conjugated DOX in saline (final concentration from 0 to 8 μg of DOX/ml or $9 \cdot 10^{-8}$—$1.5 \cdot 10^{-5}$ M) and incubated at 37 °C for 15 or 30 s (early interaction period), or 15 or 30 min (late interaction period). Upon incubation, $8 \cdot 10^4$ particles of DOX-M conjugate per cell were applied to ensure saturation of the binding sites. The observed effects on signal transduction were stimulated solely by immobilized DOX, as DOX desorption from the conjugate during the observation times was negligible (less than 0.4% over 1 hour, Fig. 2) and the conjugate did not penetrate into the cell during the experiment (Fig. 3).

The concentrations of cGMP and cAMP extracted into ethanol were determined using an «Amersham» radioimmune analysis test system and «Beckman» β counter [10]. The reference concentrations in the erythhrocytes suspension were 0.49 ± 0.17

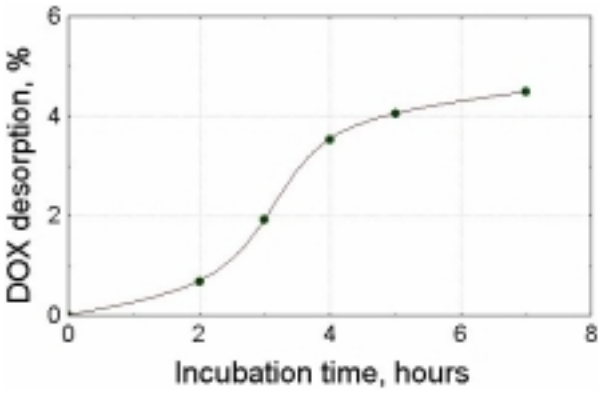

Fig. 2. DOX release profile versus incubation time for DOX-M conjugate at 37 °C in a physiological solution, pH 7.4.

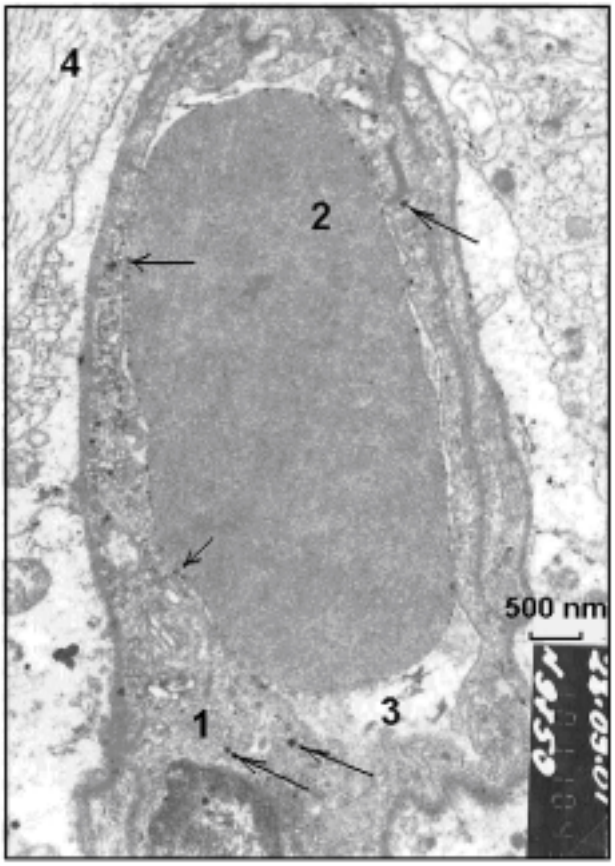

Fig. 3. Mouse cerebral cortex 1 hour after i.v. injection of 25 μg DOX-M conjugate (or 0.15 mg DOX) per g (w/w): arrows denote electron dense particles distributed in endothelial cells (1), in the blood capillary lumen (3) and in neurophyl (4), and attached to the membrane of erythrocyte (2).

and 38.3 ± 6.4 pmol/g of protein for cGMP and cAMP, respectively. Each data point represents a mean of four measurements (probe duplicates for erythrocytes from two different donors).

To determine the content of stable NO metabolite NO_2^-, the cell suspension was added to an equal volume of 1N $HClO_4$ solution, following the incubation period. NO_2^- content in deproteinized aliquots was determined using Griess reagent with Green's method [11]. Data represent the mean of twelve measurements performed in four parallel probes from three different donors for each time point. The reference concentrations in the erythhrocytes suspension were 0.600 ± 0.055 nmol/mg protein for NO_2^-.

The content of protein was determined by the Bradford method [18] using bovine serum albumin as a standard.

Erythrocyte acid resistance was determined using a kinetic method [13]. Changes in extinction were determined at 750 nm every 30 seconds throughout the hemolysis of intact and $NaNO_2$-damaged erythrocytes in the presence of different concentrations of free and conjugated DOX.

DOX-M conjugate with immobilized DOX concentration of 6.1 mg of DOX/g carrier was given as an injection of 0.1 ml suspensions into the eye sinus vein of an adult male mouse weighing approximately 20 g, in a dose of 12.5 μg of Fe/g of tissue (w/w). After 60 min animal was sacrificed, tissue samples were removed and processed for electron microscopy study. Fixation was performed in 1% glutaraldehyde in 0.1 M cacodylate buffer, pH 6.8, for 1 hour followed by treatment in 1% osmium tetroxide for an hour. Dehydration process was carried out in a series of alcohol water solutions with increasing concentration of ethyl alcohol, followed by treatment in 100% etanol and two portions of pure acetone. Impregnation was made for 1 hour in each of acetone–epoxy resin mixtures (3:1, 1:1, 1:3) and for 16–20 hours in the pure resin. For impregnation and block production the following mixture of epoxy resins was used: Araldite M, Epoxy Embedding Medium 812, Epoxy Embedding Medium DDSA, Epoxy Embedding Medium DMP 30. Ultrathin sections were cut using an ultratones "Reichert" (Germany) and LKB-III. Sections were opacificated with uranilacetat solution in 70% alcohol and with lead citrate with 15 minutes incubation in each of solutions. Ultrathin tissue sections were analysed under a JEM-100C electron microscope.

Results and Discussion

DOX immobilized at the surface of magnetite nanoparticles retained its ability to bind its target receptors in competition with free DOX.

Fig. 4 shows the binding of immobilized DOX to human erythrocytes in the presence of 10^{-12}–10^{-5} M free DOX. The introduction of free DOX inhibited immobilized DOX binding, providing evi-

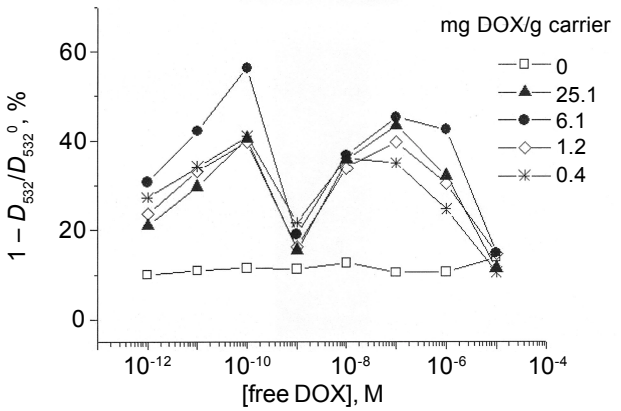

Fig. 4. Mean values of erythrocyte binding for DOX-M conjugates with ratios of immobilized DOX to free DOX in the incubation medium.

T a b l e 1. Kinetic parameters of acid hemolysis of human erythrocytes damaged with $NaNO_2$ performed in the presence of different free and immobilized DOX concentrations

[DOX], μg/ml	Stability index	t_s, min	t_t, min	$\Delta t = t_t - t_s$, min	*n*, units	t_{max}, min
			Free DOX			
0	128	0	6	6	2	0.5
0.05	455	2	10.5	8.5	3	3
0.1	552	2	11	9	4	5
0.4	675	1.5	16	14.5	8	5
2.0	699	2.5	19.5	17	7	4.5
8.0	717	2.5	17	14.5	11	6
			DOX-M conjugate			
0	505	1.5	9	7.5	4	5.5
0.05	548	0.5	12.5	12	4	5.5
0.1	602	1.5	13	11.5	5	6
0.4	614	1	20.5	19.5	8	5.6
2.0	699	1	23.5	22.5	11	5.6
8.0	626	2.5	15	11.5	7	6

Abbreviations: starting time of hemolysis, t_s; time of hemolysis termination, t_t; total duration of hemolysis, ($\Delta t = t_t - t_s$); number of erythrocyte fractions, *n*; position of the kinetic curve maximum, t_{max}.

dence of specific DOX binding at the cell surface. As shown by the concurrent binding measurements (Fig. 4), there are two highly specific binding sites (receptor pools) for DOX at the plasma membrane of human erythrocytes. 0.16–1.2 mg DOX/g carrier in a conjugate is enough to saturate binding with cell receptors, i.e. further increase in concentration the immobilized DOX causes no increase in binding the conjugate.

No specific binding with the plasma membrane was observed for the nanodispersed magnetite without immobilized DOX, however, a small amount of magnetite bound to the erythrocytes. This nonspecific binding of magnetic nanoparticles resulted in a substantial protector effect against the hemolysis of erythrocytes damaged by $NaNO_2$ treatment (Table 1, [DOX]=0).

Binding of the DOX conjugates to the erythrocyte plasma membrane was shown to occur also *in vivo*. Fig. 3 shows the ultrastructural localization of the conjugate particles in the ultrathin tissue section of the cerebral cortex of the mouse after the conjugate i.v. injection to an animal. The electron dense particles of the DOX-M conjugate attached to a mouse erythrocyte membrane in the blood capillary lumen of the cerebral cortex, distributed in endothelial cells and in neutrophyl. It can be seen that there is no penetration of the conjugate into the erythrocyte during 1 hour following the conjugate injection to an animal. According to the morphometry data the attached particle density is close to 100 particles per mm^2 of erythrocyte surface, which, when accounting for the apparent erythrocyte area (≈90 mm^2), corresponds to at least $9 \cdot 10^3$ DOX binding sites at the cell surface.

Using the SANS method, aggregates of the DOX-M nanoparticles with an R_g of 90 nm were detected immediately after introduction of the DOX-M conjugate into the erythrocyte suspension (Fig. 5, *a*). Upon incubation, SANS intensity distributions

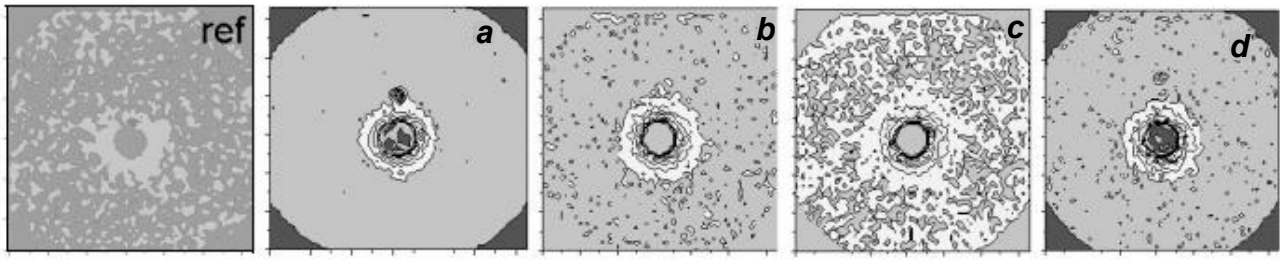

Fig. 5. 2D SANS intensity patterns, corrected for background transmission, for samples of human erythrocytes (ref) and after introduction of 3.2×10^3 DOX-M conjugate particles per cell (6.1 mg DOX per g carrier). Samples were frozen immediately (a), after 10 minutes of incubation (b), and after 30 minutes of incubation (c). The sample in (d) was preincubated for 10 minutes in the presence of 0.2 μM free DOX, then the DOX-M suspension was introduced, followed by 30 minutes of incubation and freezing. The vertical and horizontal dimensions of the plots correspond to $2q_{max}$ momentum transfer, and q_{max}=0.53 nm^{-1} (S-D=5.5 m; λ = 0.813 nm).

changed (Fig. 5, *b*, *c*) and the gyration radius of the scattering centers (DOX-M) decreased to 50 nm and 15 nm after 10 and 30 minutes of incubation, respectively, from the initial 90 nm shown in Fig. 5,*a*. The decrease in the scale of the structures is consistent with desaggregation of the DOX-M agglomerates due to interaction with erythrocytes (adsorption at the plasma membrane). Preincubation with free DOX prior to introduction of the nanomaterial resulted in the inhibition of desaggregation: R_g was estimated to be 135 nm after 30 min of incubation (Fig. 5, *d*). This result can be interpreted in terms of inhibition of the specific adsorption of the immobilized DOX-containing nanomaterial by free DOX, confirming the specific binding of the immobilized DOX preparations to the erythrocytes plasma membrane. Another important question is whether DOX binding performs a receptor function and modulates signal transduction in erythrocytes.

The effects of rapid cell activation (within 30 min) due to interaction with free and immobilized DOX were compared in the concentration range of $9 \cdot 10^{-8}$—$1.5 \cdot 10^{-5}$ M DOX. We observed immediate and similar effects of free and immobilized DOX on the formation of the second messengers (Table 2), resulting in an increase in NO_2^- and cGMP steady state concentrations and reciprocal decrease in cAMP levels (Fig. 6).

An overall significant increase in cGMP/cAMP ratio was observed (Table 3). For free and conjugated DOX, maximal [cGMP]/[cAMP] ratios were 33- and 25-fold greater, respectively, than the basal ratios at [DOX]=0. The NO_2^- level was 4.4-fold greater than basal NO_2^- level [DOX]=0. Similar changes of the tested parameters in response to free and immobilized DOX preparations provided evidence that immobilized DOX retained its ability to modulate cell signal transduction, in a similar manner to free DOX. It is also important that the termination of the cell activation occurred after 30 min of incubation.

Preparations with lower immobilized DOX concentrations (0.4 and 2 μg/ml) can be more effective than those with high concentration (8.0 μg/ml) in achieving the highest signaling effect. Interestingly, the highest specific cytotoxicity in both A2780 human ovarian carcinoma and KB human epidermoid oral cavity cancer cell lines occurred for conjugates with a DOX concentration of 6.1 mg/g of carrier, which was also one of the most effective in generating immobilized DOX signal effects (Fig. 6).

A substantial increase in NO production as a result of free and immobilized DOX signal action can be indicative of a physiological growth in intracellular Ca^{2+}-ion concentration, with subsequent constitutive NO-synthase activation. Both pathways for $[Ca^{2+}]_i$ increase are associated with activation of the phospholipid signal system. One pathway is characterized by phosphatidyl inositol hydrolyses: an increase in inositol phosphates and diacylglycerol, the second messengers responsible for the mobilization of cytoplasmic free calcium and activation of protein kinase C. It must be noted that the main conjugated calcium store in erythrocytes is in the plasma membrane (calcium is mainly associated with phosphatidyl inositol phosphates and sphingomyelin). Thus, another pathway of $[Ca^{2+}]_i$ increase is sphingomyeline hydrolysis with ceramide production. Ceramide can be further hydrolized to sphingosine, accompanied by Ca^{2+} release from the plasma membrane. Sphingosine is known to be an apoptosis trigger [14]. The increase in cGMP levels upon free and immobilized DOX signal action is apparently depend on the activation of soluble guanylate cyclase by NO. The reciprocal decrease in cAMP levels in the early period of DOX signal action can be also depend on NO increase, as NO is an inhibitor of the membrane adenylate cyclase [15].

In the investigated concentration range (0.05—8.0 μg/ml) free DOX had no hemolytic effect on intact erythrocytes membranes, and, in fact, stabilized the plasma membrane and increased the acid resistance of intact erythrocytes and $NaNO_2$—damaged erythrocytes (Fig. 7, Table 1). Sodium nitrite provokes oxidative damage of the erythrocyte plasma membrane and stroma haemoglobin, resulting in substantial membrane labilization and decreased erythrocyte acid resistance, as evidenced by the t_{max} shift to the left compared to the values characteristic of the intact washed erythrocytes. Introduction of free or conjugated DOX into the lysis medium caused a substantial dose-dependent increase in the acid resistance of damaged erythrocytes, as confirmed by the kinetic data on erythrocytes acidic hemolysis (Table 1). The increase in the erythrocyte stability index, the time of onset of hemolysis, the time to hemolysis termination and its total duration, the increase in the number of fractions in the erythrogram, and the shift of the kinetic curve maximum to the right, all imply that an increase in erythrocyte stability has occurred in the presence of free or conjugated DOX.

An important question is: to what extent are the signal effects of free and immobilized DOX responsible for the DOX cytotoxic activity observed *in vitro* and *in vivo*? Highly active isoforms of iNOS are present in many types of cells. For DOX, both activation of iNOS enzyme activity (and even the correspondent activation of gene expression) and its inhibition have been previously reported [16,17].

The role of NO in carcinogenesis has not yet been determined. Although NO has been established as a potent inducer of apoptosis in different cell types,

T a b l e 2. Levels changing of the secondary messengers cAMP, cGMP and NO in human erythrocytes incubated in the presence of different concentrations of free DOX or immobilized DOX (DOX-M conjugates) for 15 s, 30 s, 15 min and 30 min after their introduction into erythrocyte suspensions. Data were normalized to the values determined at [DOX]=0 without the addition of DOX (for free DOX) or in the presence of the carrier itself (for DOX-M conjugate)

Preparation	[DOX], μg/ml	15 s	30 s	15 min	30 min
		$[cAMP]/[cAMP]_{[DOX]=0}$ (M, n =4)			
Free DOX	0.05	0.90	0.92	0.43**	0.71
	0.10	0.80	1.24	0.46**	0.72
	0.40	0.73	0.93	0.50**	0.65
	2.00	0.64	1.12	0.62*	1.13
	8.00	0.96	0.72	0.78	1.23
DOX-M conjugates	0.05	1.01	1.04	0.77	0.77*
	0.10	0.78	0.81	0.66	0.72*
	0.40	0.91	0.67	0.49*	0.63*
	2.00	0.56	0.69	0.68	0.80
	8.00	0.69**	0.93	0.71	0.70
			$[cGMP]/[cGMP]_{[DOX]=0}$ (M, n = 4)		
Free DOX	0.05	1.3	2.3	8.6**	8.5**
	0.10	3.3**	2.5**	11.9**	12.2**
	0.40	4.4**	3.0*	17.5*	21.6*
	2.00	3.1**	2.3**	14.3*	11.9*
	8.00	2.6*	2.5	12.4*	11.8*
DOX-M conjugates	0.05	2.87**	1.63	6.52**	5.11**
	0.10	3.62**	1.77	6.76*	7.37**
	0.40	5.02*	1.80	11.54**	9.93*
	2.00	2.40	3.29	11.47**	9.48**
	8.00	1.3	2.3	8.6**	8.5**
			$[NO_2^-]/[NO_2^-]_{[DOX]=0}$ (M, n = 12)		
Free DOX	0.05	0.8	1.7**	1.9**	0.8
	0.10	0.9	2.1**	2.2**	1.1
	0.40	1.2	2.0**	2.0**	1.2
	2.00	1.8*	3.6**	2.9**	1.3
	8.00	1.9**	4.4**	2.8**	0.9
DOX-M conjugates	0.05	1.5*	2.1**	1.4	1.8**
	0.10	1.0	2.3**	1.9**	2.0*
	0.40	1.9**	2.5**	1.6*	2.0
	2.00	2.2**	3.8**	1.8*	3.1**
	8.00	3.9**	5.5**	2.2*	1.8

*$p < 0.05$, **$p < 0.01$, mean differs significantly from reference data at [DOX]=0.

contradictory effects have been reported [18]. It was shown that low NO concentrations can contribute to cell survival, whereas higher NO concentrations are pathological and promote cell destruction [19]. The final result (activation or inhibition of apoptosis) may be determined by NO concentrations and the presence of other pro-apoptotic and anti-apoptotic factors. A significant increase in the cGMP level is considered to be an apoptotic signal. Down-regulation of cAMP also results in a shift towards apoptosis. In particular, BAD is a pro-apoptotic Bax-like protein that is reversibly modulated by cAMP-mediated phosphorylation, i.e. phosphorylated BAD is unable to promote apoptosis [20]. The inhibition of NADH oxidase related to the down-regulation of cAMP in cancer cells is also associated with growth inhibition and activation of apoptosis [5].

In conclusion, there are specific binding sites for DOX at the plasma membrane of human erythrocytes. The DOX-M conjugate does not penetrate into the cell for at least an hour. It has been established that free and conjugated DOX are antagonists

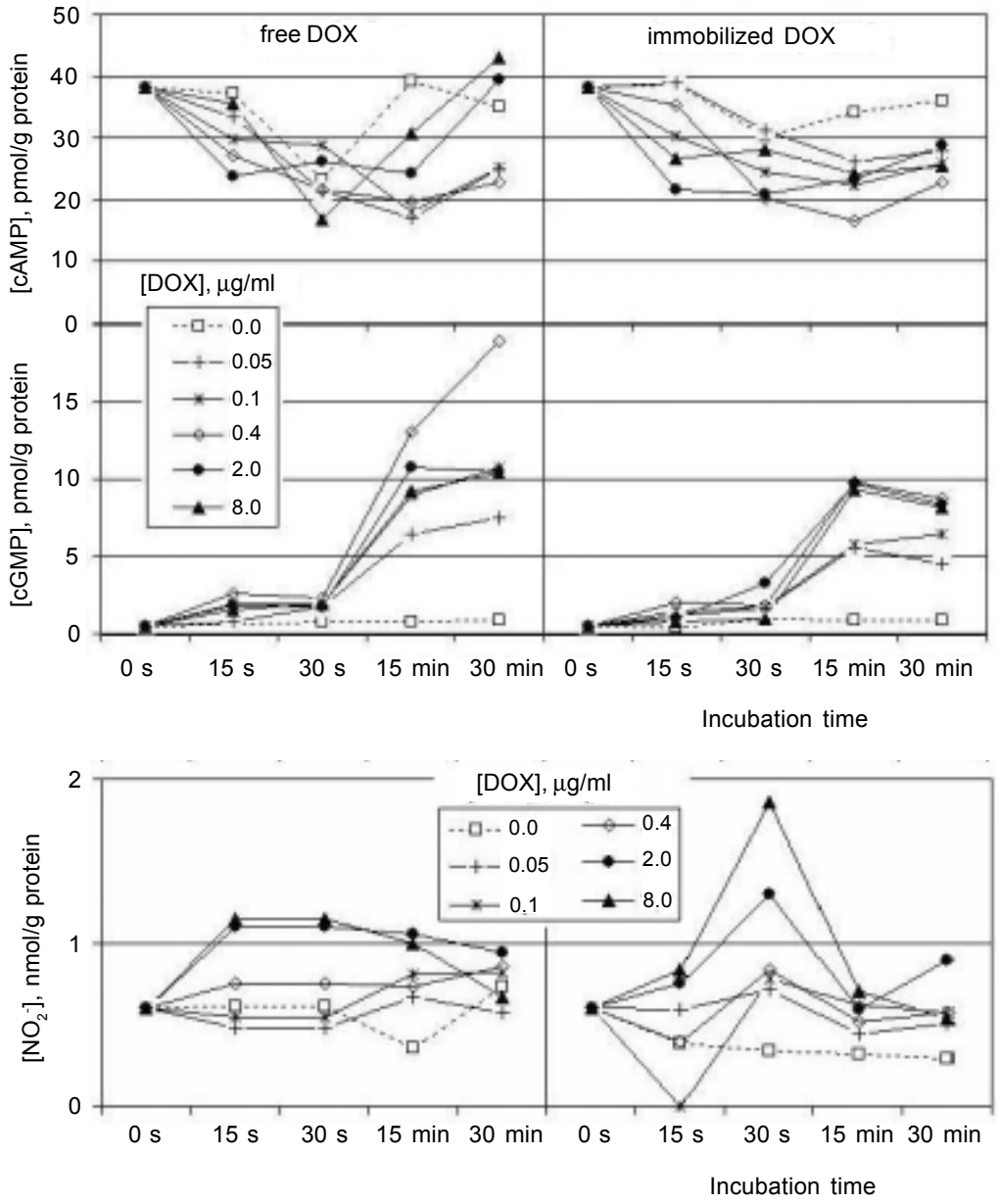

Fig. 6. Concentrations of the cyclic purine nucleotides cAMP and cGMP, and the NO metabolite NO_2^- in human erythrocytes incubated in the presence of different concentrations of free DOX or immobilized DOX (DOX-M conjugates) for 15 s, 30 s, 15 min and 30 min.

of the erythrocyte receptors coupled to the phospholipid signal system. This is evidenced by an increase in NO and cGMP levels. On the basis of the experimental data obtained, one can concede the following sequence of events initiated by DOX interaction with erythrocyte's surface (Fig. 8): DOX → → binding to receptor(s) bound to the plasma membrane → activation of phosphoinositol hydrolysis by PLC → generation of inisitoltriphosphate and diacylglycerol → increase in cytosolic calcium concentrations ($[Ca^{2+}]_i$) → activation of Ca-dependent (constitutive) NO-synthase → NO generation → activation of the cytosolic (soluble) guanylate cyclase → → cGMP generation. The decrease in cAMP levels as a consequence of DOX signalling may be caused by an increase in NO production (adenylate cyclase inhibition), or by increased cGMP levels resulting in an activation of cAMP-phosphodiesterase, which hydrolyzes cAMP with AMP production. The powerful membrane-stabilizing action of low free and conjugated DOX concentrations may signify underlying importance of membrane events in the specific anticancer action of this anthracycline antibiotic. The relative role of cell signalling in DOX anticancer

T a b l e 3. [cAMP]/[cGMP] ratio (M, n = 4) in human erythrocytes incubated in the presence of different concentrations of free DOX or immobilized DOX (DOX-M conjugates) for 15 s, 30 s, 15 min and 30 min after their introduction into erythrocyte suspensions. Data were normalized to the values determined at [DOX]=0 without the addition of DOX (for free DOX) or in the presence of the carrier itself (for DOX-M conjugate)

Preparation	[DOX], μg/ml	15 s	30 s	15 min	30 min
		$\frac{[cGMP]/[cAMP]}{([cGMP]/[cAMP)_{[DOX]=0}}$ (M, n =4)			
Free DOX	0.05	1.4	2.1	20.0*	11.1**
	0.10	4.2**	2.2	33.3*	16.7**
	0.40	5.9**	2.4	33.3*	25.0**
	2.00	3.8**	2.2	20.0*	7.1**
	8.00	2.8**	0.5	16.7*	7.1**
DOX-M conjugates	0.05	3.2*	1.0	9.1*	6.7
	0.10	5.0**	1.2	11.1*	11.1**
	0.40	6.3**	2.7*	25.0*	12.5**
	2.00	2.0	3.7**	20.0*	12.5**
	8.00	3.8*	0.8	14.3*	14.3**

*$p < 0.05$, **$p < 0.01$, mean differs significantly from reference (ref) data at [DOX]=0.

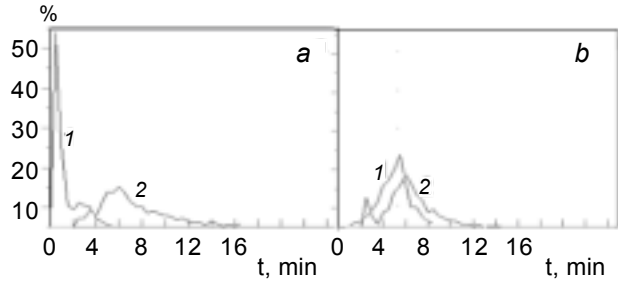

Fig. 7. Acid erythrograms of $NaNO_2$-damaged human erythrocytes. Panel (a) shows the reference curve (1) and the curve generated in the presence of 8 μg free DOX/ml (2). Panel (b) shows the curve in presence of the carrier, [DOX]=0 (1), and the curve generated in the presence of 8.0 μg immobilized DOX/ml (2).

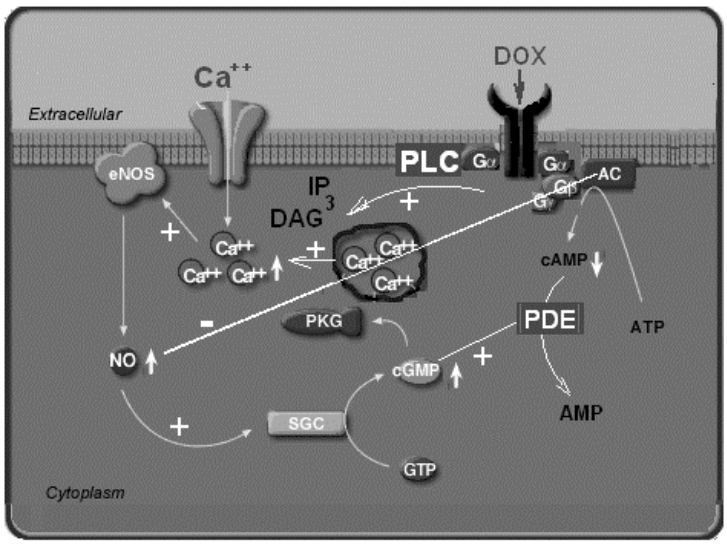

Fig. 8. Scheme of possible signal effects initiated by DOX binding at the erythrocyte's plasma membrane. Here AC − adenylyl cyclase; IP_3 − inositol 1,4,5-triphosphate, DAG − diacylglycerol, eNOS − constitutive nitric oxide synthase, PDE − phosphodiesterase, phospholipase C is PLC, PKG − protein kinase G, SGC soluble guanylate cyclase.

activity and its clinical significance is still unclear; nevertheless the features described here can suggest methods for optimization of DOX formulations.

Acknowledgments. We thank Dr. L. Stechenko for performing electron microscopy studies. We thank Dr. G. Solyanik for testing the anticancer activity of DOX conjugates in vitro and Dr. J. Gerloff for valuable discussions.

SOME SIGNAL EFFECTS IN HUMAN ERYTHROCYTES ON SPECIFIC BINDING OF FREE DOXORUBICIN AND DOXORUBICIN CONJUGATES WITH MAGNETITE NANOPARTICLES

O. M. Mykhaylyk[1], A. V. Kotsuruba[2], N. O. Dudchenko[1], G. Török[3]

[1]Institute of Applied Problems of Physics and Biophysics, National Academy of Sciences of Ukraine, Kyiv;
e-mail: olga.mykhaylik@gmx.net;
[2]Palladin Institute of Biochemistry, National Academy of Sciences, Kyiv, Ukraine;
[3]Research Institute for Solid State Physics and Optics, Budapest, Hungary;
e-mail:diu@cyfra.net

S u m m a r y

Binding of doxorubicin (DOX) immobilized on nanodispersed magnetite (DOX-M conjugates with loading in the range of 0.16–25.1 mg DOX/g carrier) to intact human erythrocytes in concurrence with free DOX was investigated. Two specific binding sites for doxorubicin were revealed at the plasma membrane of human erythrocytes. Changes in the ordering of the DOX-M nanoparticles according to small angle scattering data are consistent with their specific binding at the plasma membrane upon incubation with erythrocytes. Free and conjugated doxorubicin modulated signal transduction in erythrocytes in a similar way. Both up-regulate nitric oxide and cyclic GMP and down-regulate cyclic AMP production and stabilize the membranes of oxidatively damaged erythrocytes.

K e y w o r d s: doxorubicin (adriamycin), conjugate, human erythrocytes, plasma membrane, signal transduction, SANS, NO, cAMP, cGMP, hemolysis.

1. *Triton T. R., Yee G.* // Science. 1982. **217**. P. 248–250.
2. *Vichi P., Triton T. R.* // Cancer Res. 1992. **52**. P. 4135–4138.
3. *Cuvilier O., Nava V. E., Murtthy S. K.* // Cell Death Differ. 2001. **8**. P. 162–171.
4. *Bartolomeo S. D., Sano F. D. et al.* // J. Neurochem. 2000. **75**. P. 532–539.
5. *Morre D. J., Kim C., Paulik M. et al.* // J. Bioenerg. Biomembr. 1997. **29**. P. 269–80.
6. *Schrijvers D., Highlez M., Bruzn E. et al.* // Anti-Cancer Drugs. 1999. **10**. P. 147–153.
7. *Regev R., Eytan G. D.* // Biochem. Pharmacol. 1997. **54**. P. 1151–1158.
8. *Awasthi S., Singhal S. S., Pikula S. et al.* // Biochemistry. 1998. 37. P. 5239–5248.
9. *Mykhaylyk O., Kotzuruba A., Buchanevich O. et. al.* // J. Mang. Magn. Mater. 2001. **225**. P. 226–234.
10. *Keirus J. J., Wheeler M. A., Bitensky M. W.* // Anal. Biochem. 1974. **61**. P. 336.
11. *Green L. C., David A. W., Glogowski J. et al.* // Ibid. 1982. **126**. P. 131–138.
12. Bank N. R., Aynedjian H. S. //Kidney Int. 1993. **43**. P. 1306–1312.
13. *Терсков И. А., Гительзон И. И.* // Биофизика. 1957. **2**. С. 259–266.
14. *Cuvillier O., Nava V. E., Murthy S. K. et al.* // Cell Death Differ. 2001. 8. P. 162–171.
15. *Wang S., Yan L., Weslez R. A. et al.* // J. Biol. Chem. 1997. **272**. P. 5959–5965.
16. *Inagaki R., Taniguchi T., Sakai T.* // Gen. Pharmacol. 1999. **32**. P. 185–188.
17. *Sakai T., Muramatsu I., Hazashi N. et al.* // Gen. Pharmacol. 1996. **27**. P. 1367–1372.
18. *Beckman J. S. and W. H. Koppenol* // Am. J. Physiol. 1996. **271**. P. C1424–C1437.
19. *Shen Y. H., Wang X. L., Wilcken D. E. L.* // FEBS Letters. 1998. **433**. P. 125–131.
20. *Zha J., Harada H., Yang E. et al.* // Cell. 1996. **87**. P. 619–628.

Received 21.06.2004